Neuron, Volume *100*

Supplemental Information

Polarity Acquisition in Cortical Neurons Is Driven by Synergistic Action of Sox9-Regulated Wwp1 and Wwp2 E3 Ubiquitin Ligases and Intronic miR-140

Mateusz C. Ambrozkiewicz, Manuela Schwark, Mika Kishimoto-Suga, Ekaterina Borisova, Kei Hori, Andrea Salazar-Lázaro, Alexandra Rusanova, Bekir Altas, Lars Piepkorn, Paraskevi Bessa, Theres Schaub, Xin Zhang, Tamara Rabe, Silvia Ripamonti, Marta Rosário, Haruhiko Akiyama, Olaf Jahn, Tatsuya Kobayashi, Mikio Hoshino, Victor Tarabykin, and Hiroshi Kawabe

SUPPLEMENTARY FIGURES AND FIGURE LEGENDS

Supplementary Figure S1.

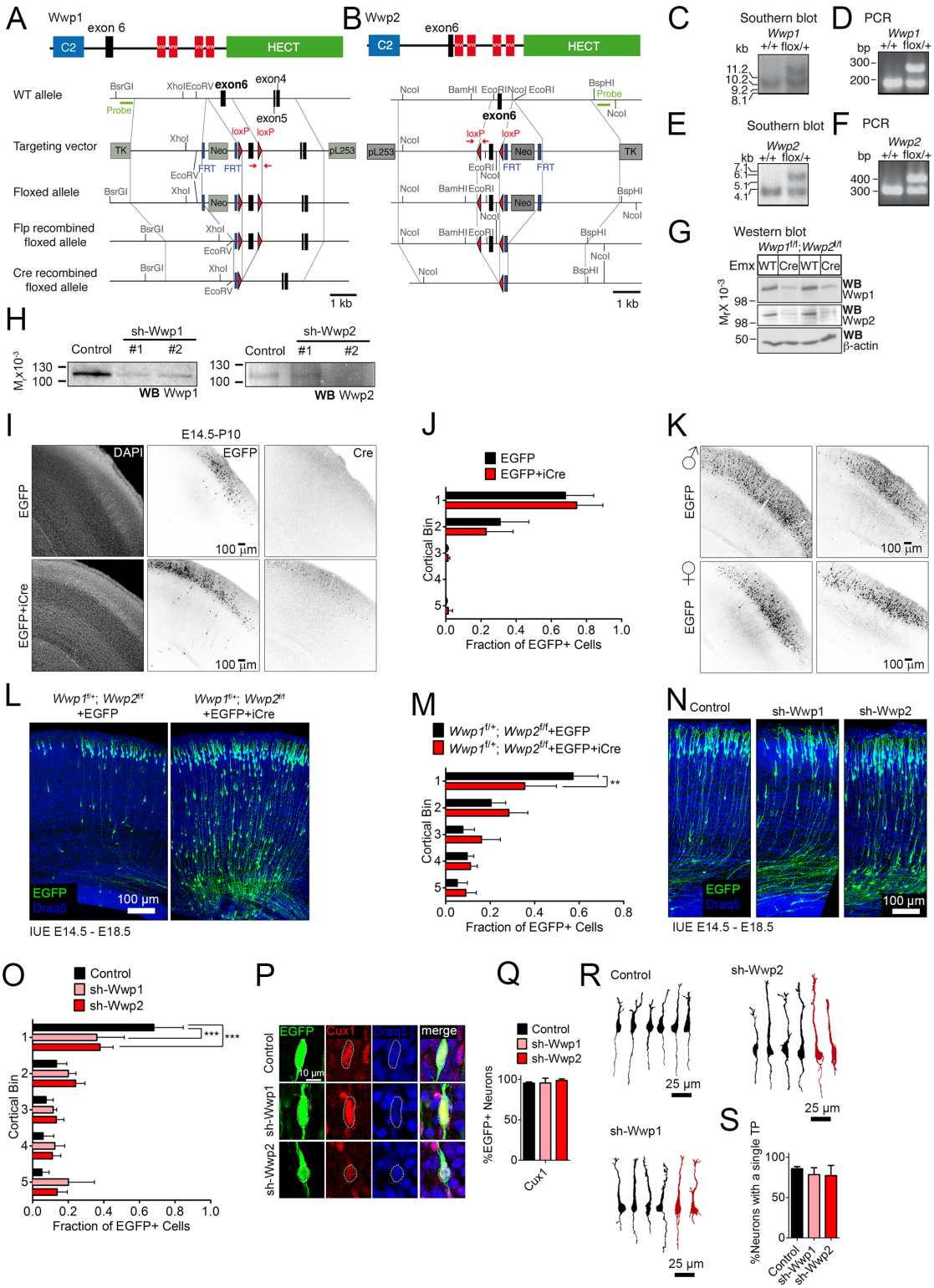

Supplementary Fig. S1. Generation and basic characterization of *Wwp1*$^{f/f}$, *Wwp2*$^{f/f}$, and *Wwp1/2*$^{f/f}$ mouse lines and sh-RNA vectors to knock down Wwp1 and Wwp2. Related to Fig. 1.

(A, B) Targeting strategies for *Wwp1* (A) and *Wwp2* (B) genes. Domain structures of Wwp1 and Wwp2 proteins (top schemes), structures of the wild type (WT) *Wwp1* and *Wwp2* alleles, Wwp1 and Wwp2 targeting vectors (Targeting vector), floxed mutant alleles (Floxed allele, Flp recombined floxed allele, and Cre recombined floxed allele) of *Wwp1* and *Wwp2*. Exons are represented as black boxes. Flp recombinase targets (FRT) and loxP sites are represented as blue rectangles and red triangles, respectively. After homologous recombination and germ line transmission of mutant alleles, *Wwp1*$^{fl/+}$ and *Wwp2*$^{fl/+}$ mice were crossed with the FLP-deleter to excise the neomycin resistance cassettes. Subsequently, exons flanked by loxP sites in mutant alleles were floxed-out by Cre. Genomic DNA fragments for Southern blotting probes are represented as green bars in WT alleles, and genotyping PCR primers are represented as red arrows in Targeting vectors. pL253, pL253 gene targeting vector; Neo, Neomycin resistance cassette; TK, herpes simplex virus thymidine kinase expression cassette. (C-G) Verification for gene targeting. (C, E) Southern blot analyses of genomic DNA samples of the WT (+/+) and targeted (flox/+) embryonic stem cells. BsrGI and NcoI were used for digestion of the genomic DNA purified from cloned embryonic stem cells of *Wwp1*$^{fl/+}$ line (C), and *Wwp2*$^{fl/+}$ line (E), respectively. 10.7 kb and 12.7 kb bands represent WT and Wwp1 floxed alleles in (C), 4.0 kb and 6.0 kb bands represent WT and Wwp2 floxed alleles in (E). (D, F) Genotyping PCR analyses of genomic DNA samples from WT (+/+) and heterozygous (flox/+) mice. (G) Western blotting in cortical lysates of P5 mice of indicated genotypes using anti-Wwp1, anti-Wwp2, and anti-β-actin antibodies. (H) Western blotting using anti-Wwp1 and anti-Wwp2 antibodies using lysates of primary cortical neuronal cultures, infected with lentiviruses expressing scramble sh-RNA (Control), sh-RNA for Wwp1 knock-down (sh-Wwp1 #1, sh-Wwp1 #2) and sh-RNA for Wwp2 knock-down (sh-Wwp2 #1, sh-Wwp2 #2). For all experiments we used sh-Wwp1 #1 and sh-Wwp2 #2. (I-K) Laminar distribution and morphology in cortical neurons are independent of Cre expression and gender in wild type mice. Related to the entire manuscript. (I) Representative images of DAPI staining, anti-EGFP immunolabeling, and anti-Cre immunolabeling in P10 cortices after IUE at E14.5 with plasmids for EGFP or for simultaneous expression of EGFP and Cre. (J) Distribution of EGFP-, and EGFP- and Cre-expressing neurons *in vivo* (Table S1G). (K) Representative images of anti-EGFP immunolabeling in P10 cortices after IUE at E14.5 with plasmids for

EGFP and myristoilated Venus expression in male and female wild type mice. Note no qualitative difference in neuronal distribution and normal pyramidal morphology. (L-S) Phenotype of the single KD of Wwp1 and Wwp2 and single *Wwp2* KO. Related to Fig. 1. (L) Representative images of EGFP immunostaining signals and Draq5 labeling in E18.5 cortices of $Wwp1^{f/+}$; $Wwp2^{f/f}$ mice electroporated *in utero* to express EGFP, or EGFP and Cre at E14.5. (M) Quantification of laminar distribution of cortical neurons in $Wwp1^{f/+}$; $Wwp2^{f/f}$ mouse brains after electroporation with EGFP, or EGFP and iCre (Table S1H). (N) Representative images of EGFP/Venus immunostaining signals and Draq5 fluorescence in E18.5 cortices of wild type mice electroporated *in utero* to express EGFP/Venus and control sh-RNA, or EGFP/Venus and sh-Wwp1, or EGFP/Venus and sh-Wwp2 at E14.5. (O) Quantification of laminar distribution of cortical neurons in mouse brains after electroporation with indicated constructs (Table S1I). (P) Representative images of immunostaining against EGFP and Cux1 antibody and Draq5 fluorescence after electroporation with indicated vectors. Cell soma is marked with a dotted line. (Q) Quantification of fraction of neurons expressing indicated vectors, positive for Cux1 (Table S1J). (R) Representative EGFP-fluorescence based tracings of neurons expressing indicated vectors. Neurons with aberrant morphology (i.e. multiple trailing processes) are colored red. (S) Quantification of the number of neurons with a single and multiple trailing process (TP) (Table S1K). Results on graphs are represented as averages ± S.D. For statistical analyses, (J), (M), (O), two-way ANOVA with Bonferroni post-hoc test; (Q) and (S), one-way ANOVA with Bonferroni post-hoc test. *** $p < 0.001$; ** $0.001 < p < 0.01$.

Supplementary Figure S2.

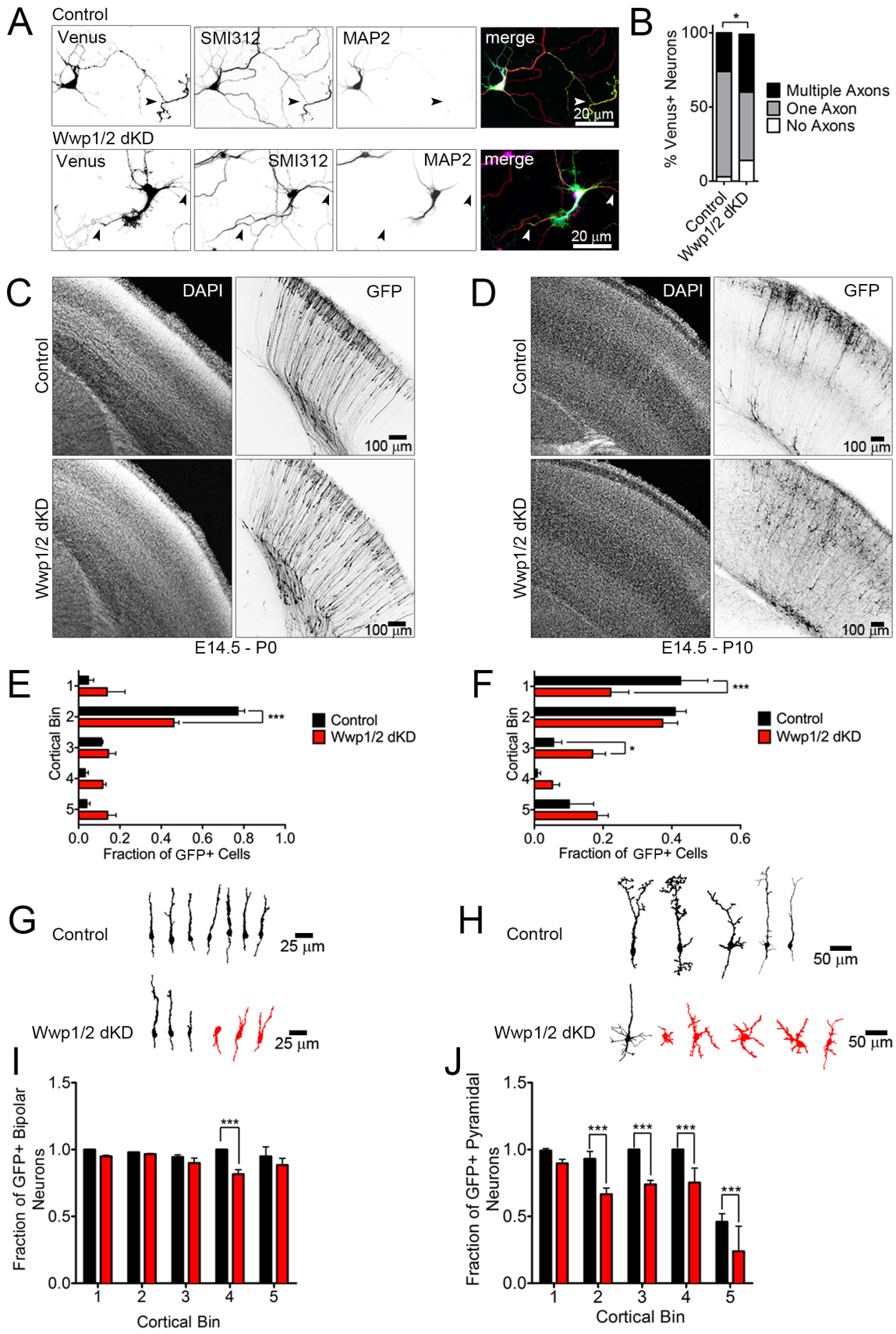

Supplementary Fig. S2. Induction of multiple axons, aberrant distribution and morphology of cortical neurons upon Wwp1 and Wwp2 double knock-down. Related to Fig. 1.

(A) Representative images of cultured primary hippocampal neurons transfected with plasmid encoding control scramble sh-RNA, or with two plasmids encoding sh-RNAs for double knock-down of Wwp1 and Wwp2 (Wwp1/2 dKD). Neurons were transfected at DIV1 and fixed at DIV7. Arrowheads indicate axons positive for SMI312 and negative for MAP2 staining. (B) Quantification of the number of axons projected from a single neuron. Quantification of the number of axons projected by a single neuron (Table S1L). (C-J) Cortical progenitors of wild type mice were transfected *in utero* at E14.5 with a plasmid encoding myristoilated Venus (myr-Venus) and control non-silencing sh-RNA, or co-transfected with two plasmids, one encoding myr-Venus together with sh-RNA to downregulate Wwp1, and another one encoding myr-Venus and sh-RNA for Wwp2. Brains were then fixed at P0 (C, E, G, I), and at P10 (D, F, H, J). (C, D) Representative maximum intensity projections of 100 μm thick Z-stacks of DAPI signals and immunostaining with anti-GFP antibody in coronal cryosections. (E, F) Distribution of control and Wwp1/2 dKD neurons in P0 (E) or P10 (F) cortex. Images of cortices were divided into 5 bins of identical dimensions and the relative number of neurons was counted in each bin (Table S1M and S1N). (G, H) Representative morphologies of neurons in bin 3 and 4 of P0 (G) or P10 (H) control or Wwp1/2 dKD brains. (I) Quantification of neuronal polarities. Numbers of BP neurons were counted in each cortical bin (Table S1O). (J) Fractions of pyramidal neurons in control and Wwp1/2 dKD in P10 cortices. Relative numbers of neurons with a single prominent dendritic shaft projecting towards the pia in each bin were expressed as averages ± S.D. (Table S1P). Results on graphs are represented as averages ± S.D. For statistical analyses, (B), Chi-square test; (E), (F), (I), (J), two-way ANOVA. *** $p < 0.001$; ** $0.001 < p < 0.01$; * $p < 0.05$.

Supplementary Figure S3.

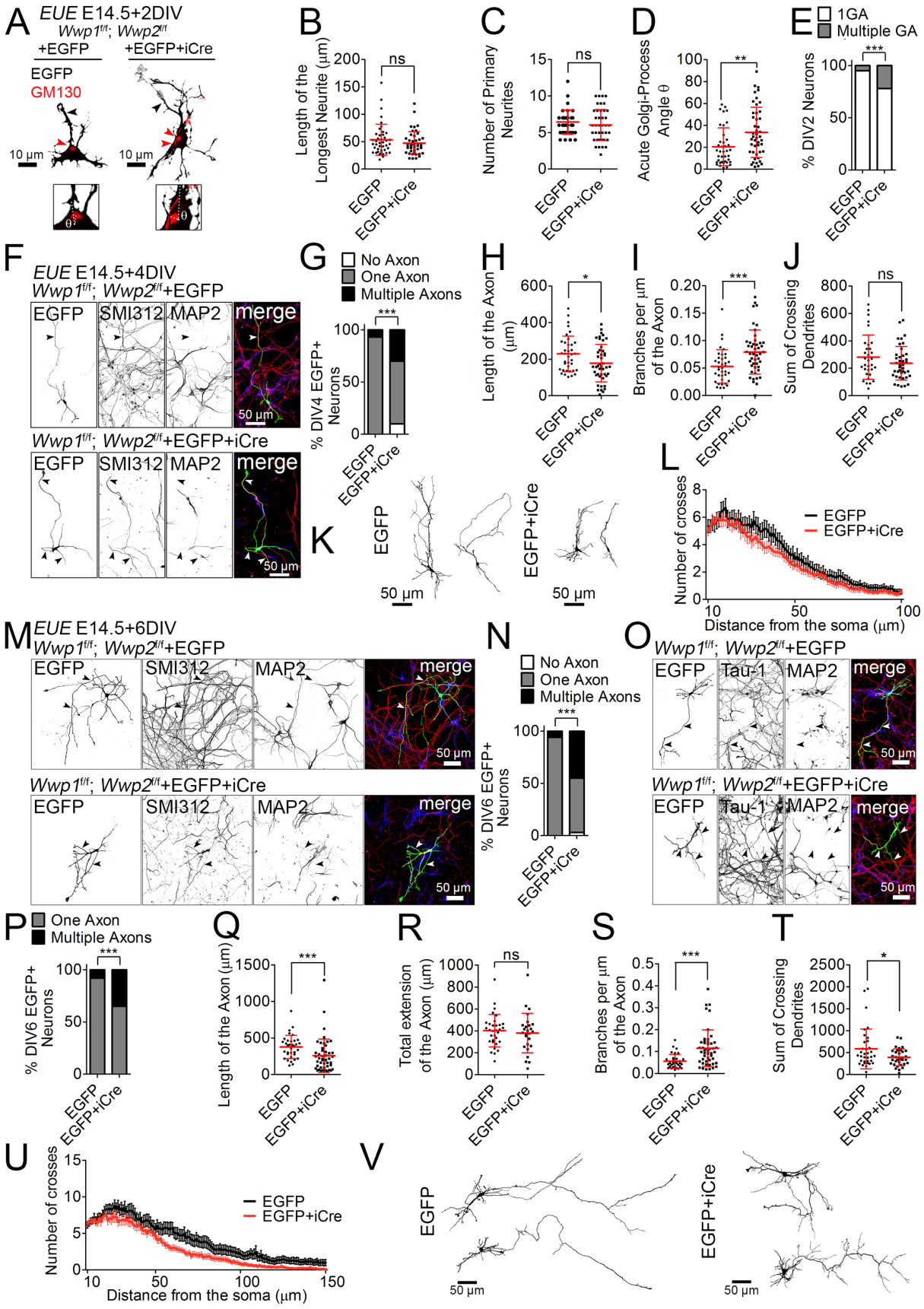

Supplementary Fig. S3. Double knock-out of *Wwp1* and *Wwp2* induces multiple axons and aberrances in neurite growth in cortical primary neurons. Related to Fig. 1.

(A) Images of representative primary cortical *Wwp1/2*$^{f/f}$ neurons after *ex utero* electroporation (EUE) at E14.5. Control neurons expressing EGFP and *Wwp1/2* dKO expressing GFP and Cre recombinase were fixed at DIV2, and immunostained for EGFP and cis-Golgi marker protein GM130. Black arrowheads indicate the longest neurite, red arrowheads point to Golgi apparatus (GA). Quantification of the length of the longest neurite (Table S1Q) (B), the number of primary branches (Table S1R) (C), and the acute angle of Golgi apparatus and the emergence of the longest neurite θ (Table S1S) (D). (E) Quantification of the number of Golgi apparatus (GA) stacks in a single neuron (Table S1T). (F) Images of representative primary cortical *Wwp1/2*$^{f/f}$ neurons after EUE at E14.5. Control neurons expressing EGFP and *Wwp1/2* dKO expressing GFP and Cre recombinase were fixed at DIV4, and immunostained for axonal (SMI312) and dendritic (MAP2) marker proteins. Arrowheads indicate axons. (G) Quantification of the number of axons projected from a single neuron (Table S1U). Quantification of the length (Table S1V) (H) and branching (Table S1W) (I) of the axon, identified as SMI312-positive and Map2-negative neurite. (J) Quantification of the sum of crossings of neurites with Sholl circles in control and *Wwp1/2* dKO neurons (Table S1X). (K) Representative reconstructions of DIV4 control and *Wwp1/2* dKO neurons, based on EGFP fluorescence. (L) Sholl analysis diagram of DIV4 control and *Wwp1/2* dKO neurons. Axons were manually removed from the analysis. (M to P) Polarity of neurons estimated by two axonal markers, SMI312 and Tau-1. (M, O) Images of representative primary cortical *Wwp1/2*$^{f/f}$ neurons after EUE at E14.5. Control neurons expressing EGFP and *Wwp1/2* dKO neurons expressing GFP and Cre recombinase were fixed at DIV6, and immunostained for axonal (SMI312 in M; Tau-1 in O) and dendritic (MAP2) marker proteins. Arrowheads indicate axons. (N, P) Quantification of the number of axons, defined as Map2-negative and SMI-312-positive (Table S1Y) (N), or Tau-1-positive (Table S1Z) (P) neurite, projected from a single neuron. Quantification of the length (Table S1A') (Q), total extension (Table S1B') (R) and branching (Table S1C') (S) of the axon, identified as SMI312-, or Tau-1-positive and Map2-negative neurite. (T) Quantification of the sum of crossings of neurites with Sholl circles in control and *Wwp1/2* dKO neurons (Table S1D'). (U) Sholl analysis diagram of DIV6 control and *Wwp1/2* dKO neurons. Axons were manually removed from the analysis. (V) Representative reconstructions of DIV6 control and *Wwp1/2* dKO neurons after EUE at E14.5. Results on (L) and (U) are represented as averages ± S.E.M. Results on other graphs are represented as averages ± S.D. For statistical analyses, (B to D), (I), (Q to S), D'Agostino-

Pearson normality test and Mann-Whitney test; (H), (J), (T), D'Agostino-Pearson normality test and unpaired t-test; (E), (P), Fisher's exact test; (G), (N), Chi-square test. *** $p < 0.001$; 0.001 **$0.001 < p < 0.01$; * $0.01 < p < 0.05$.

Supplementary Fig. S4.

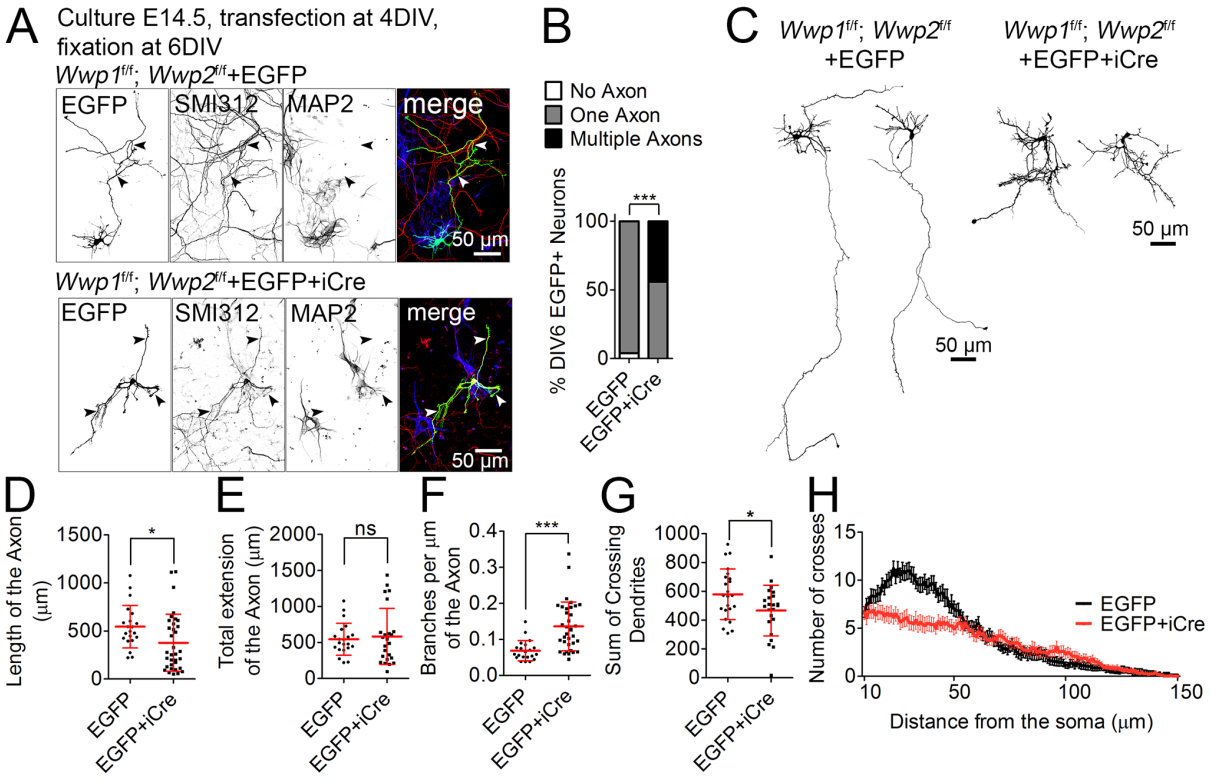

Supplementary Fig. S4. Double knock-out of *Wwp1* and *Wwp2* after initial axon specification induces multiple axons in cortical primary neurons. Related to Fig. 1.

(A) Images of representative primary cortical *Wwp1/2*$^{f/f}$ neurons. Neurons were transfected at DIV4. Control neurons expressing EGFP and *Wwp1*/2 dKO expressing GFP and Cre recombinase were fixed at DIV6, and immunostained for axonal (SMI312) and dendritic (MAP2) marker proteins. Arrowheads indicate axons. (B) Quantification of the number of axons, defined as Map2-negative and SMI-312-positive neurite, projected from a single neuron (Table S1E'). (C) Representative reconstructions of DIV6 control and *Wwp1/2* dKO neurons after transfection with EGFP or EGFP and Cre expression vectors at DIV4. Quantification of the length (Table S1F') (D), extension (Table S1G') (E), and branching (Table S1H') (F) of the axon, identified as SMI312-, or Tau-1-positive and Map2-negative neurite. (G) Quantification of the sum of crossings of neurites with Sholl circles in control and *Wwp1/2* dKO neurons (Table S1I'). (H) Sholl analysis diagram of DIV6 control and *Wwp1/2* dKO neurons. Axons were manually removed from the analysis. Results on (H) are represented as averages ± S.E.M. Results on other graphs are represented as averages ± S.D. For statistical analyses, (B), Chi-square test; (D-F), D'Agostino-Pearson normality test and Mann-Whitney test; (G), D'Agostino-Pearson normality test and unpaired t-test. *** $p < 0.001$; * $0.01 < p < 0.05$.

Supplementary Fig. S5.

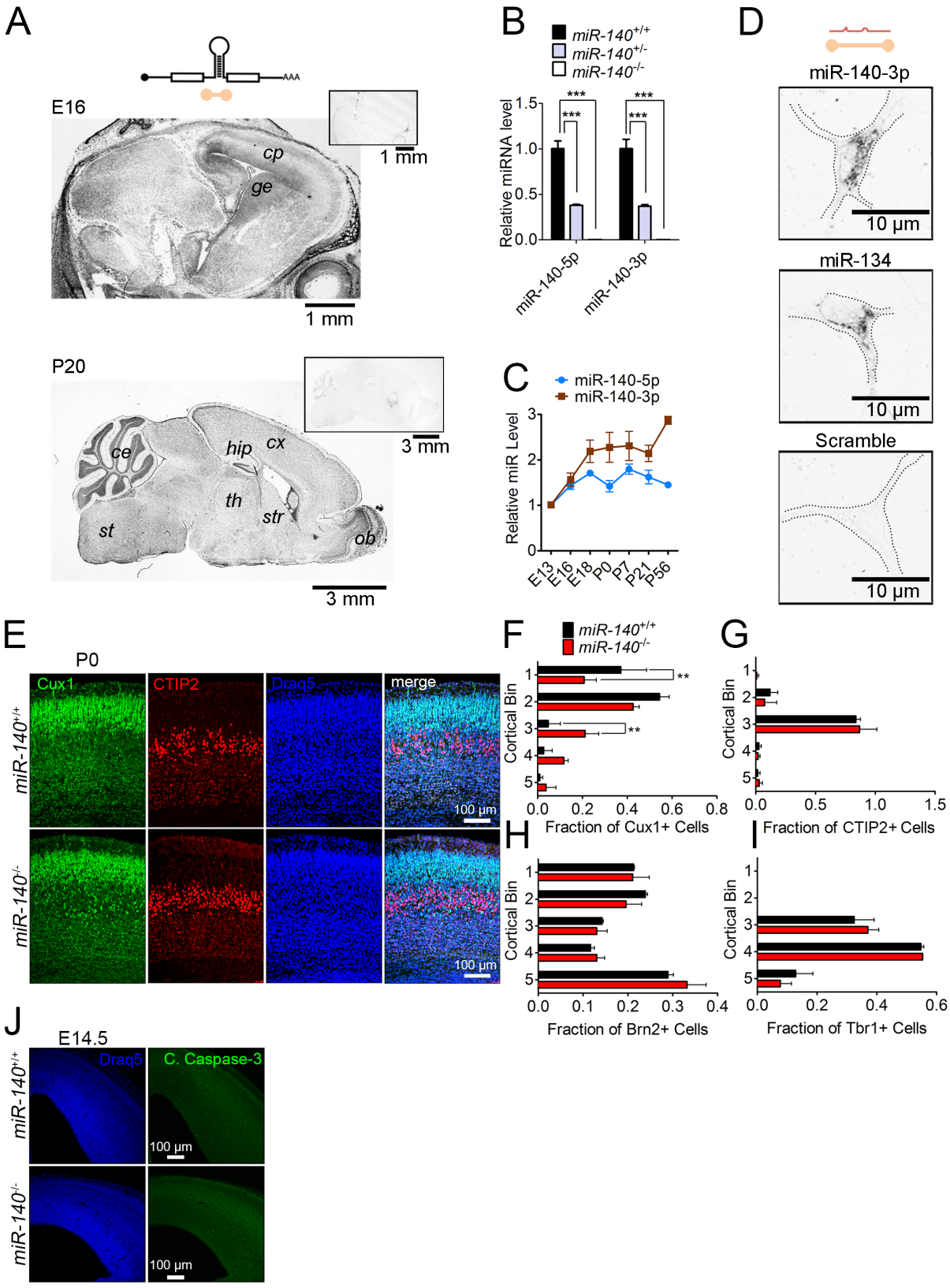

Supplementary Fig. S5. miR-140 is expressed in murine central nervous system and its knock-out engenders aberrant lamination of Cux1-positive neurons. Related to Fig. 2.

(A) Results of *in situ* hybridization of the antisense probe for intronic *miR-140* spanning *Wwp2* locus (upper scheme) on sagittal sections of E16 and P20 wild type mouse brain. Images in the top right inserts represent signals from the control sense probe; cortical plate (cp), ganglionic eminence (ge); cortex (cx), hippocampus (hip), cerebellum (ce), brain stem (st), thalamus (th), striatum (str) and olfactory bulb (ob). (B) Validation of qRT-PCR primer specificity for miR-140-5p and -3p. cDNA samples were prepared from total RNA extracted from cerebral cortices of *miR-140*$^{+/+}$, *miR-140*$^{+/-}$, and *miR-140*$^{-/-}$ mice at P21. The level of each miR-140 strand was expressed relative to component of spliceosome, U6 snRNA - RNU6B (Table S1J'). (C) Developmental profile of miR-140-3p and -5p expression in developing mouse cortex. Total RNA was isolated from cortices of mice of depicted ages. The level of each miRNA strand was expressed relative to RNU6B and to the miR level at E13 (Table S1K'). (D) *In situ* hybridization with locked-nucleic acid probes (upper scheme) for mature miR-140-3p (top panel), dendritic miR-134 (middle panel), and scramble control (bottom panel) in DIV7 primary hippocampal neurons. Edges of cell bodies are outlined with black dotted lines. (E) Representative images of immunostaining against Cux1, CTIP2 and Draq5 labeling in P0 *miR-140*$^{+/+}$ or *miR-140*$^{-/-}$ cortices. (F-I) Quantification of laminar distribution of cortical neurons positive for indicated fate markers in *miR-140*$^{+/+}$ or *miR-140*$^{-/-}$ mouse brains (Tables S1O' – S1R'). (F), Cux1; (G), CTIP2; (H), Brn2, expressed in neuronal progenitors and upper layer neurons; and (I), Tbr1, a deeper layer neuron marker. (J) Representative images of immunostaining against cleaved caspase-3 and Draq5 labeling in P0 *miR-140*$^{+/+}$ or *miR-140*$^{-/-}$ cortices. Results on (C) are represented as averages ± S.E.M. Results on (B) and (F-I) are represented as averages ± S.D. For statistical analyses, (B) one-way ANOVA with Bonferroni post-hoc test; (F-I) two-way ANOVA with Bonferroni post-hoc test. *** $p < 0.001$; ** $0.001 < p < 0.01$.

Supplementary Fig. S6.

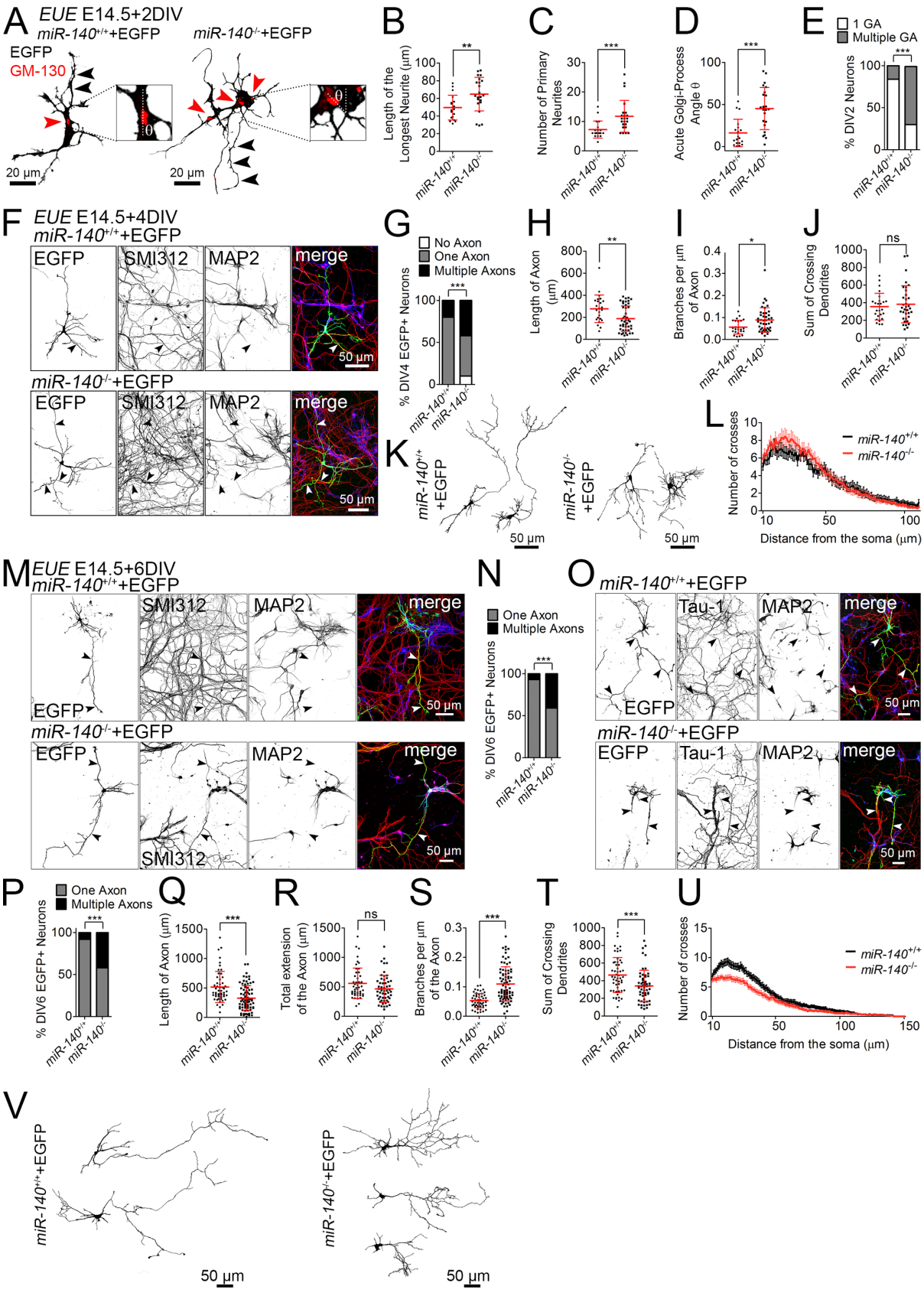

Supplementary Fig. S6. Knock-out of *miR-140* induces multiple axons and aberrances in neurite growth in cortical primary neurons. Related to Fig. 2.

(A) Images of representative primary cortical *miR-140*$^{+/+}$ and *miR-140*$^{-/-}$ neurons after EUE at E14.5. Neurons of both genotypes expressing EGFP were fixed at DIV2, and immunostained for EGFP and cis-Golgi marker protein GM130. Black arrowheads indicate the longest neurite, red arrowheads point to Golgi apparatus (GA). Quantification of the length of the longest neurite (Table S1V') (B), the number of primary neurites (Table S1W') (C), and the acute angle of Golgi apparatus and the emergence of the longest neurite θ (Table S1X') (D). (E) Quantification of the number of Golgi apparatus (GA) stacks in a single neuron (Table S1Y'). (F) Images of representative primary cortical *miR-140*$^{+/+}$ and *miR-140*$^{-/-}$ neurons after EUE at E14.5. Neurons of both genotypes expressing EGFP were fixed at DIV4, and immunostained for axonal (SMI312) and dendritic (MAP2) marker proteins. Arrowheads indicate axons. (G) Quantification of the number of axons projected from a single neuron (Table S1Z'). Quantification of the length (Table S1A") (H) and branching (Table S1B") (I) of the axon, identified as SMI312-positive and Map2-negative neurite. (J) Quantification of the sum of crossings of neurites with Sholl circles in control and *miR-140* KO neurons (Table S1C"). (K) Representative reconstructions of DIV4 control and *miR-140* KO neurons, based on EGFP fluorescence. (L) Sholl analysis diagram of DIV4 control and *miR-140* KO neurons. Axons were manually removed from the analysis. (M and O) Images of representative primary cortical *miR-140*$^{+/+}$ and *miR-140*$^{-/-}$ neurons after EUE at E14.5. Neurons of both genotypes expressing EGFP were fixed at DIV6, and immunostained for axonal (SMI312 in M; Tau-1 in O) and dendritic (MAP2) marker proteins. Arrowheads indicate axons. (N, P) Quantification of the number of axons, defined as Map2-negative and SMI-312-positive (N), or Tau-1-positive (P) neurite, projected from a single neuron (Table S1D" and S1E"). Quantification of the length (Table S1F") (Q), extension (Table S1G") (R), and branching (Table S1H") (S) of the axon, identified as SMI312-, or Tau-1-positive and Map2-negative neurite. (T) Quantification of the sum of crossings of neurites with Sholl circles in control and *miR-140* KO neurons (Table S1I"). (U) Sholl analysis diagram of DIV6 control and *miR-140* KO neurons. Axons were manually removed from the analysis. (V) Representative reconstructions of DIV6 *miR-140*$^{+/+}$ and *miR-140*$^{-/-}$ neurons after EUE at E14.5. Results on (L) and (U) are represented as averages ± S.E.M. Results on other graphs are represented as averages ± S.D. For statistical analyses, (B), (D), D'Agostino-Pearson normality test and unpaired t-test; (C), (H to J), (Q to T), D'Agostino-Pearson normality test and Mann-Whitney

test; (E), (N), (P), Fisher's exact test; (G), Chi-square test. *** $p < 0.001$; ** $0.001 < p < 0.01$; * $0.01 < p < 0.05$.

Supplementary Fig. S7.

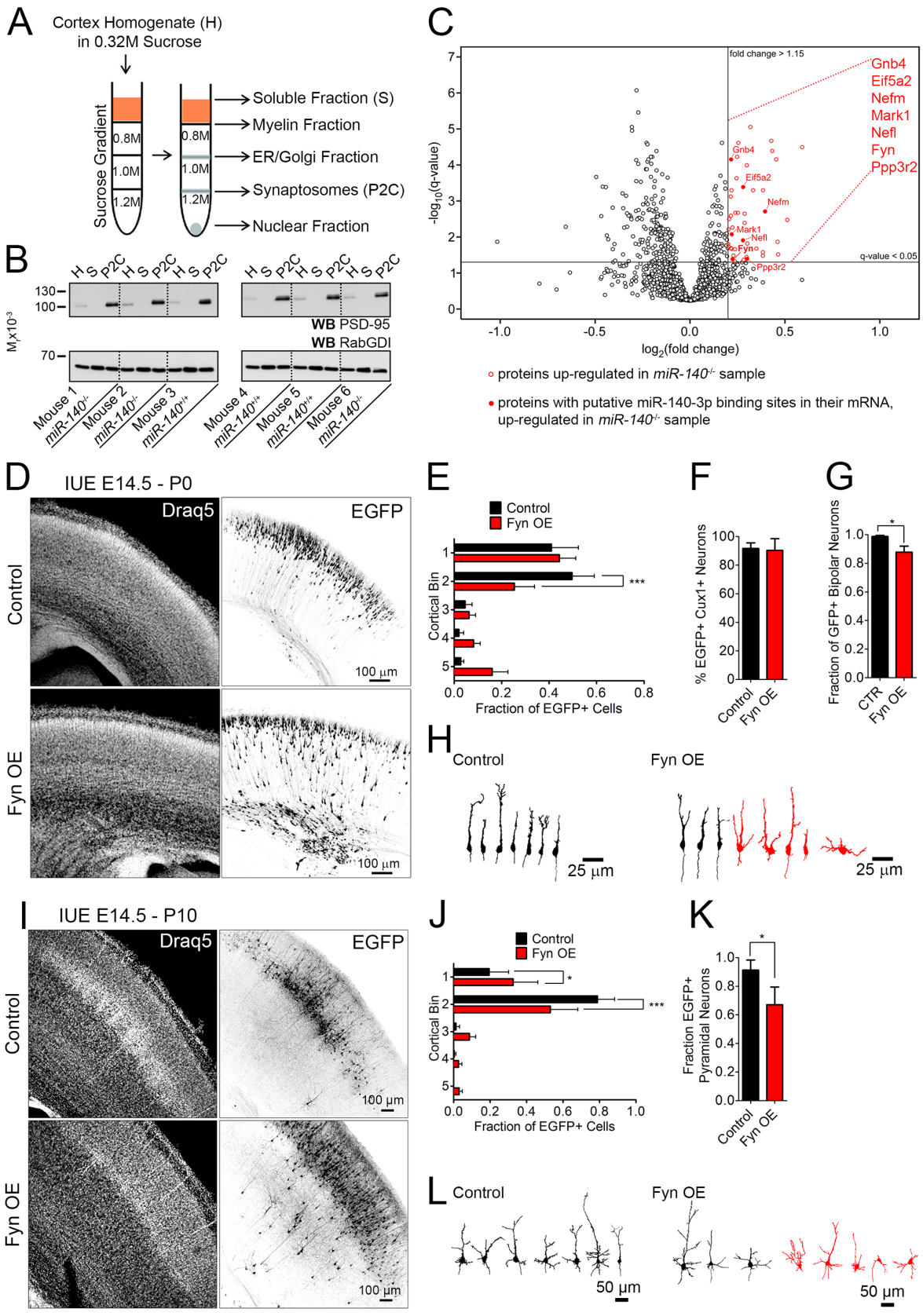

Supplementary Fig. S7. Identification of miR-140 downstream targets and overexpression of Fyn in wild type neurons resembles the loss of miR-140 in migrating cortical neurons. Related to Fig. 3.

(A) Schema of synaptosome purification from *miR-140*$^{+/+}$ and *miR-140*$^{-/-}$ mouse brains. Homogenate (H), Soluble fraction (S), and Synaptosome fraction (P2C) were used in validation in (B). (B) Validation of synaptosomal preparation by Western blotting using anti-PSD-95 and anti-RabGDI antibodies. Same protein amounts of H, S, and P2C were loaded for SDS-PAGE. Note enrichment of PSD-95 in synaptosomes (P2C), and persistent levels of RabGDI in all fractions. (C) Volcano plot with proteins identified by quantitative proteomics. Putative targets of miR-140 are listed in red, the $\log_2$ fold-change of protein level in *miR-140*$^{-/-}$ samples relative to *miR-140*$^{+/+}$ samples, and the corresponding q-values of moderated t-statistics with false discovery-based correction for multiple comparisons. q-values < 0.05 were considered significant. Proteins with fold change > 1.15 and with putative miR-140-3p binding sites along their 3'UTR were selected as putative miR-140 targets. (D) Representative images of Draq5 fluorescence and EGFP immunofluorescence in P0 cortices. Cortical progenitors of wild type mice were transfected *in utero* at E14.5 to express GFP (Control), or simultaneously over-express EGFP and Fyn (Fyn OE). (E) Distribution of Control and Fyn overexpressing (OE) neurons (Table S1R"). (F) Quantification of Cux1-positive neurons relative to total number of control or Fyn OE cells (Table S1S"). (G) Quantification of Control and Fyn OE neurons with BP morphology (Table S1T"). (H) Representative morphologies of Control and Fyn OE neurons in bin 3 and 4 at P0. Neurons with aberrant, non-BP morphology are colored red. (I) Representative images of EGFP immunostaining signals and Draq5 labeling in P10 cortices of mice electroporated *in utero* to express EGFP, or EGFP and Fyn overexpression vector (Fyn OE) at E14.5. (J) Quantification of laminar distribution of cortical neurons in mouse brains after electroporation with EGFP or EGFP and Fyn overexpression vector (Table S1U"). (K) Quantification of the number of neurons with a pyramidal morphology (Table S1V"). (L) Representative EGFP-fluorescence based tracings of neurons expressing indicated vectors. Neurons with aberrant, non-pyramidal morphology are colored red. Results on graphs are represented as averages ± S.D. For statistical analyses, (F), (G), (K), unpaired t-test; (E), (J), two-way ANOVA with Bonferroni post-hoc test. *** $p < 0.001$; * $0.01 < p < 0.05$.

Supplementary Fig. S8.

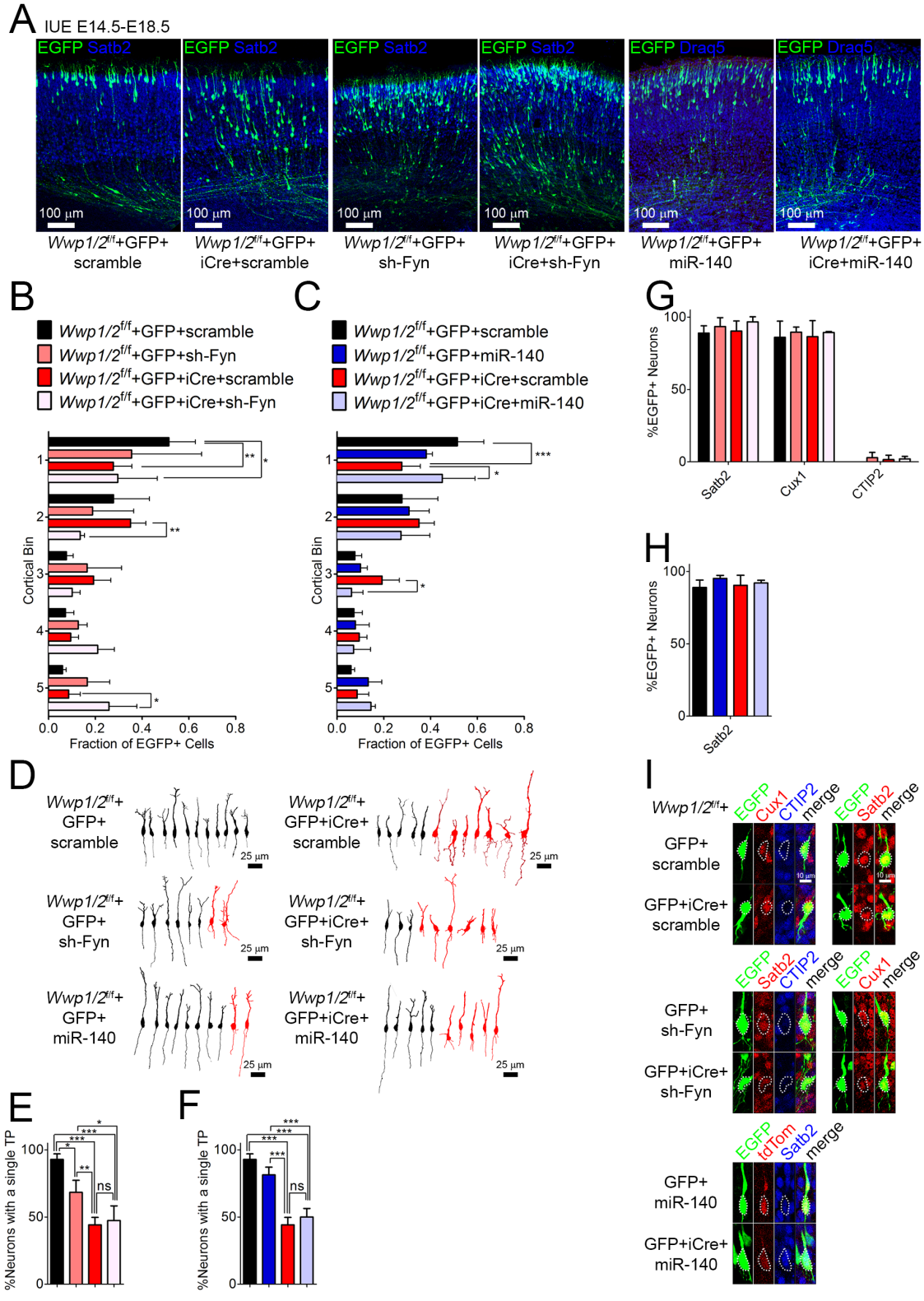

Supplementary Fig. S8. Wwp1/2 operate in Fyn-independent manner. Related to Fig. 1, 2, 3, and 4.

(A) Representative images of immunostaining against EGFP and Satb2 or Darq5 labeling in E18.5 *Wwp1/2*$^{f/f}$ cortices electroporated *in utero* at E14.5 to express indicated vector combinations. (B, C) Quantification of laminar distribution of cortical neurons in *Wwp1/2*$^{f/f}$ mouse brains after electroporation with indicated vectors (Table S1A''' and S1B'''). (D) Representative EGFP-fluorescence based tracings of *Wwp1/2*$^{f/f}$ neurons expressing indicated vectors. Neurons with aberrant morphology (i.e. multiple trailing processes) are colored red. (E, F) Quantification of the number of neurons with a single trailing process (TP) (Table S1C''' and S1D'''). Legends for the graphs are on panel (B, C). (G) Quantification of the fraction of EGFP-positive *Wwp1/2*$^{f/f}$ neurons expressing indicated fate markers after IUE with vectors indicated on (B) (Table S1E'''). (H) Quantification of the fraction of EGFP-positive *Wwp1/2*$^{f/f}$ neurons expressing Satb2 after IUE with vectors indicated on (C) (Table S1F'''). (I) Representative images of immunostaining against EGFP, Cux1, CTIP2, Satb2, and tdTomato after IUE with indicated vectors. tdTomato is a reporter used to visualize expression of miR-140. Cell soma is marked with a dotted line. Results on graphs are represented as averages ± S.D. For statistical analyses, (B) and (C), two-way ANOVA with Bonferroni post-hoc test; (E-H), one-way ANOVA with Bonferroni post-hoc test. *** $p < 0.001$; ** $0.001 < p < 0.01$.

Supplementary Fig. S9.

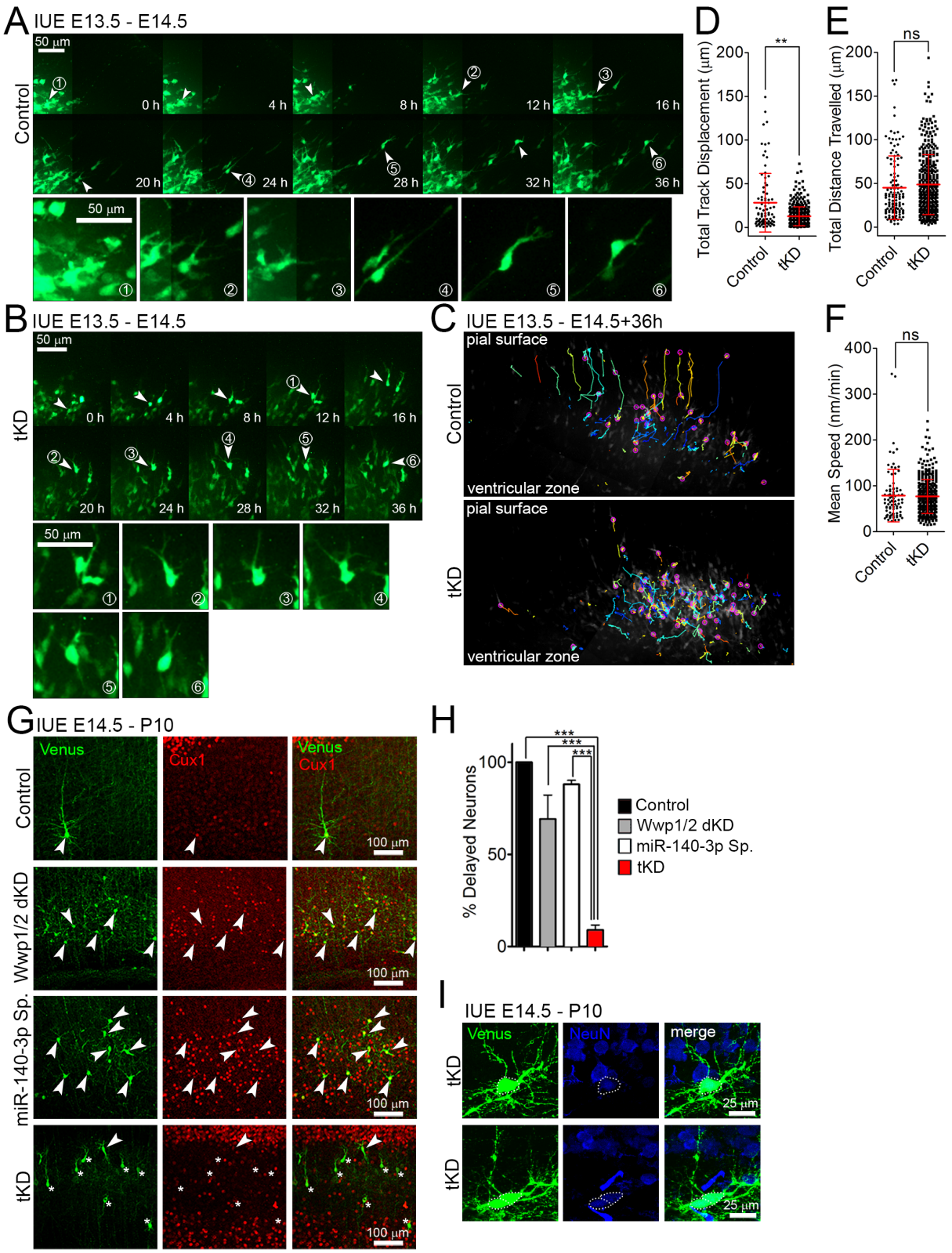

Supplementary Fig. S9. Wwp1/2 and miR-140-3p triple knock-down neurons translocate in a non-radial fashion and lose their terminal differentiation marker expression. Related to Fig. 4.

(A) Montage of a representative control neuron. Arrowhead points to one neuron over the course of 36 hours-long imaging experiment. Magnifications of respective cell states are depicted under pictures 1-6 on the bottom panel. (B) Montage of a representative tKD neuron. Arrowheads point to a single neuron. Magnifications of respective cell states are depicted under pictures 1-6 on the bottom panel. Neuronal progenitors at E13.5 were *in utero* electroporated with vectors encoding for non-silencing sh-RNA and control sponge (A), or with plasmids for the expression of sh-RNAs to downregulate Wwp1 and Wwp2 and miR-140-3p-Sponge (tKD) (B). Slice culture was prepared at E14.5 and images of developing cortical plate were taken every 30 minutes using spinning disc confocal microscope. (C) Representative reconstruction of tracks of control and tKD neurons. (D to F) Quantifications of (D) total track displacement (Table S1N'''), (E) total distance travelled (Table S1O'''), (F) and the mean speed of movement (Table S1P''') of control or tKD neurons. (G) Immunolabeling with anti-GFP antibody and anti-Cux1 antibodies in Wwp1/2 dKD, miR-140-3p-Sponge-expressing, and Wwp1/2; miR-140-3p tKD P10 cortices after IUE at E14.5. Presented is a fragment of bin 3 of cortical coronal cryosection. Arrowheads point to Venus- and Cux1-positive neurons. Asterisks mark neurons positive for Venus and negative for Cux1. (H) Quantification of Cux1-positive neurons delayed in deeper cortical layers in control and upon Wwp1/2 dKD, miR-140-3p-Sponge expression, or Wwp1/2; miR-140-3p tKD. (Table S1Q'''). (I) EGFP/myrVenus-expressing tKD neurons (green) are positive for a neuronal marker NeuN (blue). Cell soma is highlighted by the dashed line. Results on graphs are represented as averages ± S.D. For statistical analyses, (D-F), D'Agostino and Pearson omnibus normality test and Mann Whitney test; (H), one-way ANOVA with Bonferroni post-hoc test. *** $p < 0.001$; ** $0.001 < p < 0.01$.

Supplementary Fig. S10.

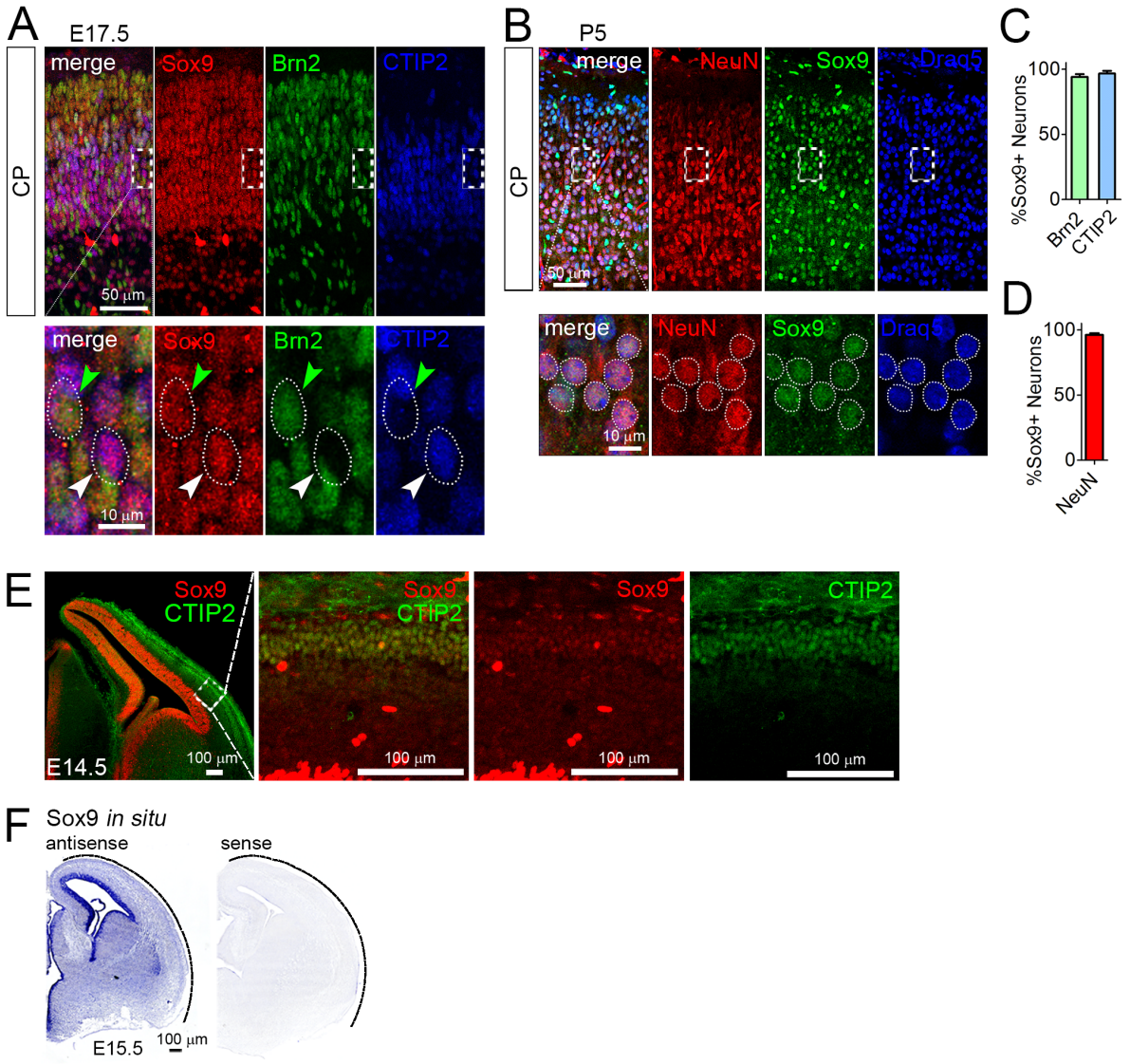

Supplementary Fig. S10. Sox9 is expressed in the ventricular zone and postmitotic neurons of the cortical plate. Related to Fig. 5.

(A) Representative images of immunostaining signals in E17.5 cortical plate (CP) of wild type mice to visualize expression of Sox9, Brn2 and CTIP2. White arrowhead points to CTIP2+ Sox9+ neuron, green arrowhead points to Brn2+ Sox9+ neuron. Cell nucleus is marked with a dotted line. (B) Representative images of immunostaining signals in P5 cortical plate (CP) of wild type mice to visualize expression of NeuN, Sox9, and and Draq5 labeling. Cell nucleus is outlined with a dotted line. (C) Quantification of fraction of Brn2+ or CTIP2+ neurons that express Sox9 (Table S1S'''). (D) Quantification of NeuN+ neurons that express Sox9 (Table S1T'''). (E) Immunohistochemistry in E14.5 brain coronal cryosection with antibodies for Sox9 and CTIP2, a marker for deeper layer postmitotic neurons. Note that CTIP2 positive neurons are also positive for Sox9 (F) Results of *in situ* hybridization on E15.5 coronal cryosection of embryonic brain using an antisense and sense probe for *Sox9*. Bars on (C-D) represent averages ± S.D.

Supplementary Fig. S11.

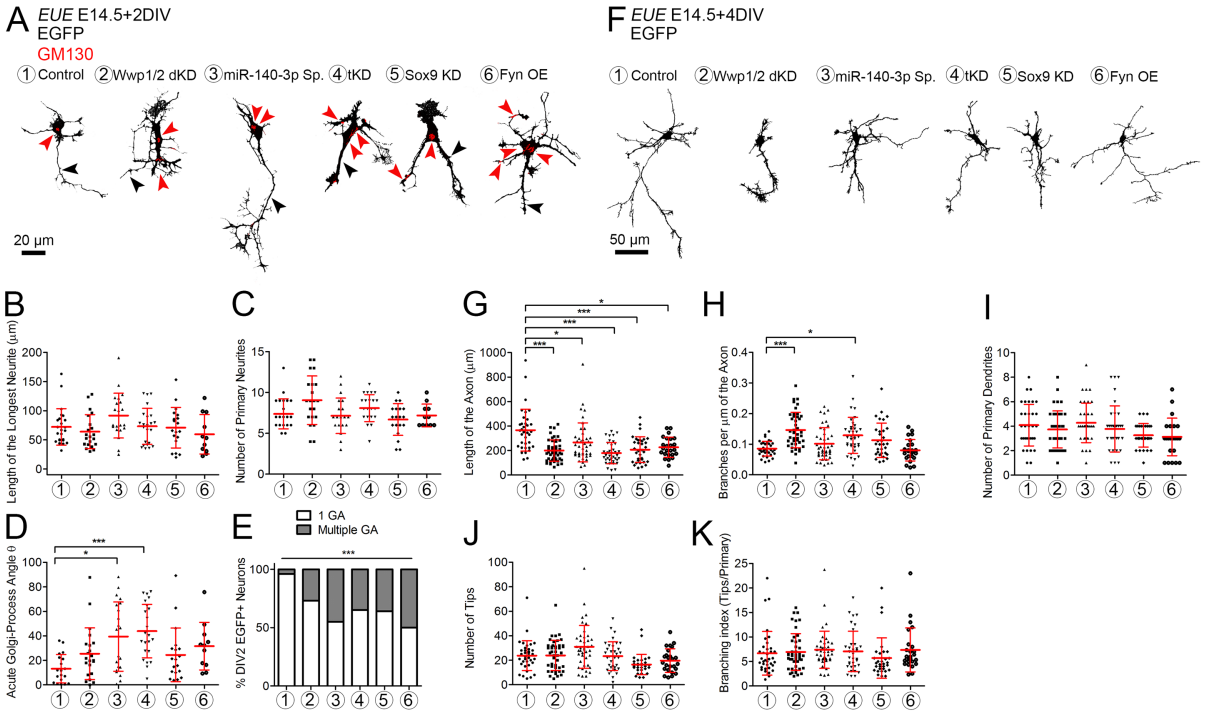

Supplementary Fig. S11. Development of cortical neurons upon disruption to Sox9-Wwp1/2-miR-140-Fyn pathway. Related to Fig. 6, 7, and 8.

(A) Images of representative primary cortical neurons after *ex utero* electroporation (EUE) at E14.5 with indicated plasmids. (1) Control: plasmids encoding EGFP+scramble-sh-RNA-Venus+Control Sponge+mock DNA; (2) Wwp1/2dKD: EGFP+sh-RNA-Wwp1+sh-RNA-Wwp2-Venus+Control Sponge+mock DNA; (3) miR-140-3p Sponge: EGFP+scramble-sh-RNA-Venus+miR-140-3p Sponge+mock DNA; (4) tKD: EGFP+ sh-RNA-Wwp1+sh-RNA-Wwp2-Venus +miR-140-3p Sponge+mock DNA; (5) Sox9 KD: EGFP+sh-RNA-Sox9-Venus+Control Sponge+mock DNA; (6) Fyn OE: EGFP+scramble-sh-RNA-Venus+Control Sponge+Fyn overexpression plasmid. (A to E) Neurons expressing indicated vectors were fixed at DIV2, and immunostained for EGFP and cis-Golgi marker protein GM130. (A) Representative images of neurons at DIV2. Black arrowheads indicate the longest neurite, red arrowheads point to Golgi apparatus (GA). Quantification of the length of the longest neurite (Table S1L"") (B), the number of primary branches (Table S1M"") (C), and the acute angle of Golgi apparatus and the emergence of the longest neurite θ (Table S1N"") (D). (E) Quantification of the number of Golgi apparatus (GA) stacks in a single neuron (Table S1O""). (F to K) Neurons expressing indicated vectors were fixed at DIV4, and immunostained for EGFP. (F) Representative images of neurons at DIV4. (G) Quantification of the length of axon identified as a neurite expressing SMI312 or Tau-1 and negative for MAP2 (Table S1P""). (H) Quantification of axon branching (Table S1Q""), (I) number of primary dendrites (Table S1R""), (J) number of dendritic tips (Table S1S""), (K) branching index as a ration between the number of dendritic tips and number of primary dendrites in a single neuron (Table S1T""). Results on (B to D) and (G to K) are represented as averages ± S.D. For statistical analyses, (B to D) and (G to K), D'Agostino and Pearson omnibus normality test and Kruskal-Wallis test with Dunn's Multiple comparison test; (E), Chi-square test. *** $p < 0.001$; ** $0.001 < p < 0.01$; * $0.01 < p < 0.05$.

Supplementary Fig. S12.

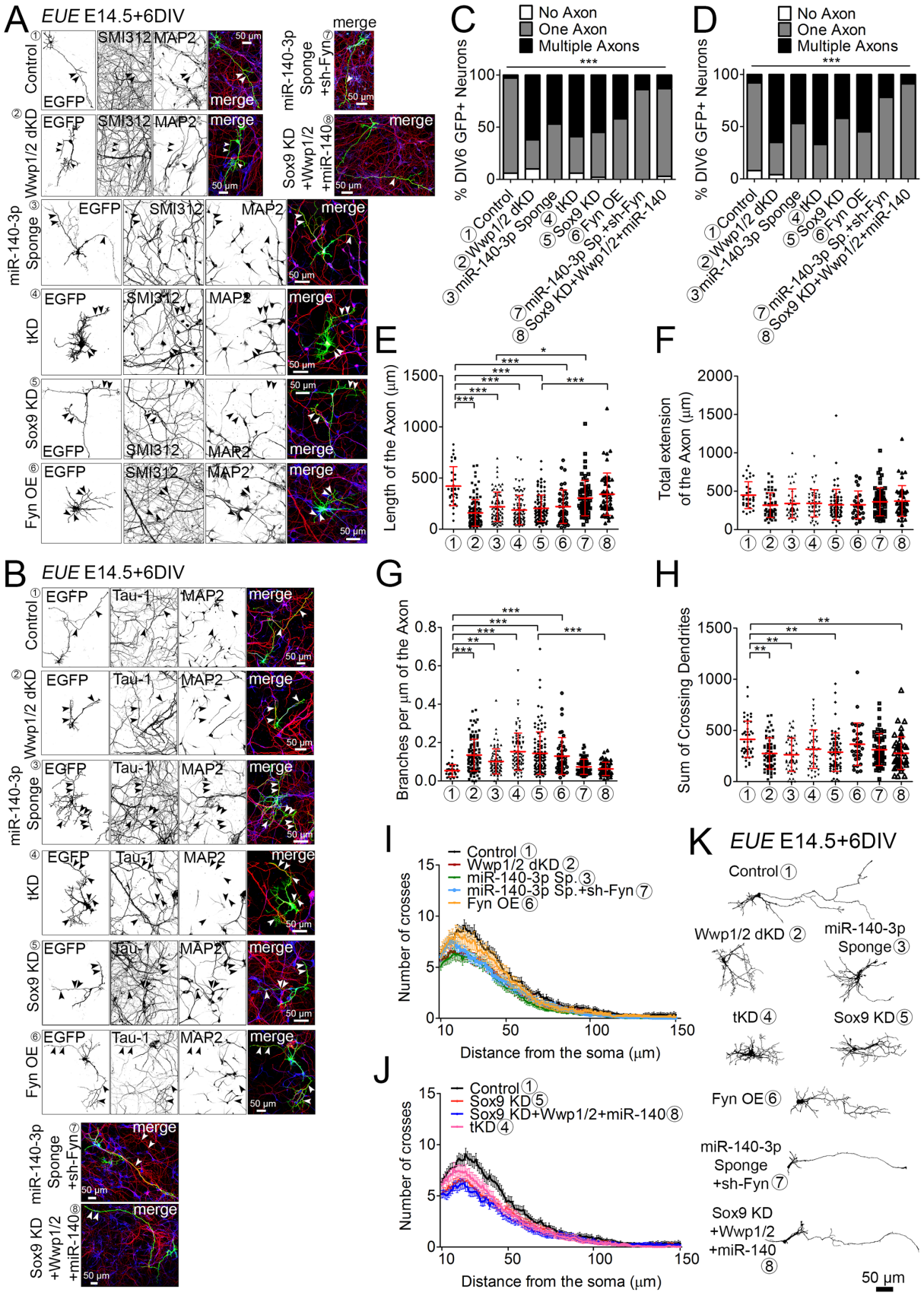

Supplementary Fig. S12. Induction of multiple axons and aberrances to axon-dendrite growth upon disruption to Sox9-Wwp1/2-miR-140-Fyn pathway. Related to Fig. 7 and 8.

(A, B) Images of representative primary cortical neurons after *ex utero* electroporation (EUE) at E14.5 with indicated vectors. (1) Control: plasmids encoding EGFP+scramble-sh-RNA-Venus+Control Sponge+mock DNA; (2) Wwp1/2dKD: EGFP+sh-RNA-Wwp1+sh-RNA-Wwp2-Venus+Control Sponge+mock DNA; (3) miR-140-3p Sponge: EGFP+scramble-sh-RNA-Venus+miR-140-3p Sponge+mock DNA; (4) tKD: EGFP+ sh-RNA-Wwp1+sh-RNA-Wwp2-Venus +miR-140-3p Sponge+mock DNA; (5) Sox9 KD: EGFP+sh-RNA-Sox9-Venus+Control Sponge+mock DNA; (6) Fyn overexpression (OE): EGFP+scramble-sh-RNA-Venus+Control Sponge+Fyn overexpression plasmid; (7) miR-140-3p Sp.+sh-Fyn: EGFP+sh-RNA-Fyn +miR-140-3p Sponge+mock DNA; (8) Sox9KD+Wwp1/2+mIR-140: EGFP+sh-RNA-Sox9-Venus+Control Sponge+Wwp1 OE+Wwp2 OE+miR-140 OE plasmids. Neurons were fixed at DIV6, and immunostained for axonal marker SMI312 (A) or Tau-1 (B) and dendritic MAP2 proteins. Arrowheads indicate axons. (C, D) Quantification of the number of axons, defined as MAP2-negative and (C) SMI-312-, or (D) Tau-1-positive neurite, projected from a single neuron, Chi square tests (Tables S1U"" and S1V""). Quantification of the length of the axon defined as a SMI312- or Tau-1-positive an MAP2-negative neurite (Table S1W"") (E), total extension of the axon defined as total length of all axons projected from a single neuron (Table S1X"") (F), branching of the axon (Table S1Y"") (G), and total number of crossing dendrites with Sholl circles (Table S1Z"") (H). (I, J) Sholl analysis diagrams of DIV6 primary cortical neurons expressing indicated vectors. Axons were manually removed from the analysis. (K) Representative EGFP-based tracings of primary cortical neurons after EUE at E14.5 with indicated vectors. Results on (E-H) are represented as averages ± S.D. Results on (I, J) are represented as averages ± S.E.M. For statistical analyses, (E), (G), (H), D'Agostino and Pearson omnibus normality test and Kruskal-Wallis test with Dunn's Multiple comparison test; (F), D'Agostino and Pearson omnibus normality test and one-way ANOVA with Bonferroni post-hoc test; (C and D), Chi-square test. *** $p < 0.001$; ** $0.001 < p < 0.01$; * $0.01 < p < 0.05$.